Steel and Composite Structures, *Vol. 21, No. 1 (2016) 123-136*
DOI: http://dx.doi.org/10.12989/scs.2016.21.1.123

Static analysis of the FGM plate with porosities

R. Benferhat [*1], T. Hassaine Daouadji [2,3], L. Hadji [2,3] and M. Said Mansour [1]

[1] *Laboratoire de Géomatériaux, Département de Génie Civil, Université Hassiba Benbouali de Chlef, Algérie*
[2] *Département de Génie Civil, Université Ibn Khaldoun de Tiaret, Algérie*
[3] *Laboratoire des Matériaux & Hydrologie, Université Djillali Liabès de Sidi Bel Abbes, Algérie*

(*Received March 21, 2015, Revised February 19, 2016, Accepted March 05, 2016*)

Abstract. This work focuses on the behavior of the static analysis of functionally graded plates materials (FGMs) with porosities that may possibly occur inside the functionally graded materials (FGMs) during their fabrication. For this purpose a new refined plate theory is used in this work, it contains only four unknowns, unlike five unknowns for other theories. This new model meets the nullity of the transverse shear stress at the upper and lower surfaces of the plate. The parabolic distribution of transverse shear stresses along the thickness of the plate is taken into account in this analysis; the material properties of the FGM plate vary a power law distribution in terms of volume fraction of the constituents. The rule of mixture is modified to describe and approximate material properties of the FG plates with porosity phases. The validity of this theory is studied by comparing some of the present results with other higher-order theories reported in the literature, the influence of material parameter, the volume fraction of porosity and the thickness ratio on the behavior mechanical P-FGM plate are represented by numerical examples.

Keywords: functionally graded material; higher-order theory; refined theory; volume fraction of porosity

1. Introduction

Functionally graded materials (FGMs) are new inhomogeneous materials. It is one of the most functional forms of composite structures developed by the composite industry. It has attained broad acceptance in aerospace and many other industries and it is widely employed in aircraft and space vehicles, ships, boats, cargo containers, and residential constructions. The technique of grading ceramics along with metals initiated by the Japanese material scientist in Sendai has marked the beginning of exploring the possibility of using FGMs for various structural applications (Reddy 2000).

FGMs are considered as a potential structural material for future high-speed spacecraft and power generation industries. FGMs are new materials, microscopically inhomogeneous, in which the mechanical properties vary smoothly and continuously from one surface to the other. In an FGM, the composition and structure gradually change over volume, resulting in corresponding changes in the properties of the material. By applying the many possibilities inherent in the FGM concept, it is anticipated that materials will be improved and new functions for them created.

During the last two decade there has been a considerable research reports on mechanical response, buckling, free vibration, etc. of FGM structural elements. Several studies have been

*Corresponding author, Mr., E-mail: rabiebenferhat@yahoo.fr

http://www.techno-press.org/?journal=scs&subpage=6 ISSN: 1229-9367 (Print), 1598-6233 (Online)

performed to analyze the behavior of functionally graded plates and shells. Bourada *et al*. (2015) gives a new simple shear and normal deformations theory for functionally graded beams. Carrera *et al*. (2010) investigates the static response problem of multilayered plates and shells embedding functionally graded material (FGM) layers**.** Kiani *et al*. (2012) has analyzed the static and dynamic of an FGM doubly curved panel resting on the Pasternak-type elastic foundation. Al-Basyouni *et al*. (2015) analyzed the bending and vibration of functionally graded micro beams based on modified couple stress theory and neutral surface position. Mahi *et al*. (2015) presented a new hyperbolic shear deformation theory for bending and free vibration analysis of isotropic, functionally graded, sandwich and laminated composite plates. Cinefra *et al*. (2012) presented a refined models based on the Carrera's unified formulation (CUF) for the static analysis of plates and shells made of functionally graded material (FGM), subjected to mechanical loads. Neves *et al*. (2011) presented a study using the radial basis function collocation method to analyze static deformations of functionally graded plates using a sinusoidal shear deformation plate formulation, allowing for through-the-thickness deformations. Ravikiran *et al*. (2008) have studied the static behavior of functionally graded metal–ceramic (FGM) beams under ambient temperature. Neves *et al*. (2012a) presented an original hyperbolic sine shear deformation theory for the bending and free vibration analysis of functionally graded plates, the theory accounts for through-the-thickness deformations. Sepahi *et al*. (2010) have studied the effects of three-parameter elastic foundations and thermo-mechanical loading on axisymmetric large deflection response of a simply supported annular FGM plate. Neves *et al*. (2012b) studied the static and free vibration analysis of functionally graded plates using a quasi-3D sinusoidal shear deformation theory. Hadji *et al*. (2015) proposed a refined exponential shear deformation theory for free vibration of FGM beam with porosities. Bennoun *et al*. (2016) gives a novel five variable refined plate theory for vibration analysis of functionally graded sandwich plates. However, in FGM fabrication, micro voids or porosities can occur within the materials during the process of sintering. This is because of the large difference in solidification temperatures between material constituents (Zhu *et al*. 2001). Wattanasakulpong *et al*. (2012) also gave the discussion on porosities happening inside FGM samples fabricated by a multi-step sequential infiltration technique. Therefore, it is important to take in to account the porosity effect when designing FGM structures subjected to dynamic loadings. Recently, Wattanasakulpong and Ungbhakorn (2014) studied linear and nonlinear vibration problems of elastically and restrained FG beams having porosities.

In this study, a new refined theory for static analysis of simply supported FGM plates with considering porosities that may possibly occur inside the functionally graded materials (FGMs) during their fabrication are proposed. The plates are made of an isotropic material with material properties varying in the thickness direction only. Analytical solutions for bending deflections of FGM plates are obtained. The governing equations are derived from the principle of minimum total potential energy. Numerical examples are presented to illustrate the accuracy and efficiency of the present theory and the influence of material parameter, the volume fraction of porosity and the thickness ratio on the behavior mechanical P-FGM plate.

2. Problem formulation

The FGM plate is regarded to be a single layer plate of uniform thickness. Here we ascertain the FGM plate of length a, width b and total thickness h made from anisotropic material of metal and ceramics and grading is assumed to be only through the thickness, in which the composition varies from top to bottom surface.

2.1 Higher-order plate theory

The displacements of a material point located at (x, y, z) in the plate may be written as

$$
\begin{aligned}
u(x,y,z) &= u_0(x,y) - z\frac{\partial w_0}{\partial x} + \Psi(z).\theta_x \\
v(x,y,z) &= v_0(x,y) - z\frac{\partial w_0}{\partial y} + \Psi(z).\theta_y \\
w(x,y,z) &= w_0(x,y)
\end{aligned}
\tag{1}
$$

where u, v, w are displacements in the x, y, z directions, u_0, v_0 and w_0 are midplane displacements, and θ_x and θ_y are the rotations of normal's to the midplane about the y and x axes, respectively. $\psi(z)$ represents shape function determining the distribution of the transverse shear strains and stresses along the thickness. The displacement field of the classical thin plate theory (CPT) is obtained easily by setting $\psi(z) = 0$. The displacement of the first-order shear deformation plate theory (FSDPT) is obtained by setting $\psi(z) = z$. Also, the displacement of parabolic shear deformation plate theory (PSDPT) of (Reddy 1984) is obtained by setting

$$\Psi(z) = z\left(1 - \frac{4z^2}{3h^2}\right) \tag{2a}$$

$$\Psi(z) = z\left(1 - \frac{4z^2}{3h^2}\right) \tag{2b}$$

In addition, the exponential shear deformation plate theory (ESDPT) of Karama *et al*. (2003) is obtained by setting

$$\Psi(z) = ze^{-2\left(\frac{z}{h}\right)^2} \tag{2c}$$

2.2 Present refined sinusoidal shear deformation plate theory

Unlike the other theories, the number of unknown functions involved in the present Refined Sinusoidal Shear Deformation Plate Theory (RSSDPT) is only four, as against five in case of other shear deformation theories (Reddy 1984, Karama *et al*. 2003). The theory presented is variationally consistent, does not require shear correction factor, and gives rise to transverse shear stress variation such that the transverse shear stresses vary parabolically across the thickness satisfying shear stress free surface conditions.

2.2.1 Basic assumptions

Assumptions of the present refined plate theory are as follows (Sid Ahmed Houari *et al*. 2013):

- The displacements are small in comparison with the plate thickness and, therefore, strains involved are infinitesimal.
- The transverse displacement W includes two components of bending w_b, and shear w_s. These components are functions of coordinates x, y, and time t only.

$$w(x,y,z) = w_b(x,y) + w_s(x,y) \tag{3a}$$

- The transverse normal stress σ_z is negligible in comparison with in-plane stresses σ_x and σ_y.
- The displacements U in x direction and V in y direction consist of extension, bending, and shear components.

$$u = u_0 + u_b + u_s \qquad v = v_0 + v_b + v_s \tag{3b}$$

The shear components u_s and v_s give rise, in conjunction with w_s, to the parabolic variations of shear strains γ_{xz} , γ_{yz} and hence to shear stresses τ_{xz} , τ_{yz} through the thickness of the plate in such a way that shear stresses τ_{xz} , τ_{yz} are zero at the top and bottom faces of the plate. Consequently, the expression for us and v_s can be given as

$$u_s = -\left(z - \sin\left(\frac{\pi z}{h}\right)\right)\frac{\partial w_s}{\partial x} \qquad v_s = -\left(z - \sin\left(\frac{\pi z}{h}\right)\right)\frac{\partial w_s}{\partial y} \tag{3c}$$

2.2.2 Displacement fields and strains

The displacement field can be obtained as follows

$$\begin{aligned} u(x,y,z) &= u_0(x,y) - z\frac{\partial w_b}{\partial x} - f(z)\frac{\partial w_s}{\partial x} \\ v(x,y,z) &= v_0(x,y) - z\frac{\partial w_b}{\partial y} - f(z)\frac{\partial w_s}{\partial y} \\ w(x,y,z) &= w_b(x,y) + w_s(x,y) \end{aligned} \tag{4}$$

And

$$f(z) = z - \sin\left(\frac{\pi z}{h}\right) \tag{5}$$

The linear strains can be obtained as

$$\begin{aligned} \varepsilon_x &= \varepsilon_x^0 + z\,k_x^b + f(z)\,k_x^s \\ \varepsilon_y &= \varepsilon_y^0 + z\,k_y^b + f(z)\,k_y^s \\ \gamma_{xy} &= \gamma_{xy}^0 + z\,k_{xy}^b + f(z)\,k_{xy}^s \\ \gamma_{yz} &= g(z)\,\gamma_{yz}^s \\ \gamma_{xz} &= g(z)\,\gamma_{xz}^s \\ \varepsilon_z &= 0 \end{aligned} \tag{6}$$

Where

$$\begin{aligned} &\varepsilon_x^0 = \frac{\partial u_0}{\partial x}, \quad k_x^b = -\frac{\partial^2 w_b}{\partial x^2}, \quad k_x^s = -\frac{\partial^2 w_s}{\partial x^2} \\ &\varepsilon_y^0 = \frac{\partial v_0}{\partial y}, \quad k_y^b = -\frac{\partial^2 w_b}{\partial y^2}, \quad k_y^s = -\frac{\partial^2 w_s}{\partial y^2} \\ &\gamma_{xy}^0 = \frac{\partial u_0}{\partial y} + \frac{\partial v_0}{\partial x}, \quad k_{xy}^b = -2\frac{\partial^2 w_b}{\partial x \partial y}, \quad k_{xy}^s = -2\frac{\partial^2 w_s}{\partial x \partial y} \end{aligned} \tag{7}$$

$$\gamma_{yz}^{s} = \frac{\partial w_s}{\partial y}, \qquad \gamma_{xz}^{s} = \frac{\partial w_s}{\partial x},$$
$$g(z) = 1 - f'(z) \quad \text{and} \quad f'(z) = \frac{df(z)}{dz} \tag{7}$$

It should be noted that the above strains are derived for geometrically linear problems. For elastic and isotropic FGMs, the constitutive relations can be written as

$$\begin{Bmatrix} \sigma_x \\ \sigma_y \\ \tau_{xy} \end{Bmatrix} = \begin{bmatrix} Q_{11} & Q_{12} & 0 \\ Q_{12} & Q_{22} & 0 \\ 0 & 0 & Q_{66} \end{bmatrix} \begin{Bmatrix} \varepsilon_x \\ \varepsilon_y \\ \gamma_{xy} \end{Bmatrix}$$
$$\begin{Bmatrix} \tau_{yz} \\ \tau_{zx} \end{Bmatrix} = \begin{bmatrix} Q_{44} & 0 \\ 0 & Q_{55} \end{bmatrix} \begin{Bmatrix} \gamma_{yz} \\ \gamma_{zx} \end{Bmatrix} \tag{8}$$

Where $(\sigma_x, \sigma_y, \tau_{xy}, \tau_{xz}, \tau_{yz})$ and $(\varepsilon_x, \varepsilon_y, \gamma_{xy}, \gamma_{xz}, \gamma_{yz})$ are the stress and strain components, respectively.

Stiffness coefficients, Q_{ij} can be expressed as

$$Q_{11} = Q_{22} = \frac{E(z)}{1-\nu^2} \qquad Q_{12} = \frac{\nu E(z)}{1-\nu^2} \qquad Q_{44} = Q_{55} = Q_{66} = \frac{E(z)}{2(1+\nu)} \tag{9}$$

2.2.3 Effective material properties of metal ceramic functionally graded plates

A FG plate made from a mixture of two material phases, for example, a metal and a ceramic. The material properties of FG plates are assumed to vary continuously through the thickness of the plate. In this investigation, the imperfect plate is assumed to have porosities spreading within the thickness due to defect during production. Consider an imperfect FGM with a porosity volume fraction, α ($\alpha \ll 1$), distributed evenly among the metal and ceramic, the modified rule of mixture proposed by Wattanasakulpong and Ungbhakorn (2014) is used as (Hadji *et al*. 2015)

$$P = P_m \left(V_m - \frac{a}{2}\right) + P_c \left(V_c - \frac{a}{2}\right) \tag{10}$$

Now, the total volume fraction of the metal and ceramic is: $V_m + V_c = 1$, and the power law of volume fraction of the ceramic is described as

$$V_c = \left(\frac{z}{h} + \frac{1}{2}\right)^k \tag{11}$$

Hence, all properties of the imperfect FGM can be written as (Hadji *et al*. 2015)

$$P = (P_c - P_m)\left(\frac{z}{h} + \frac{1}{2}\right)^k + P_m - (P_c + P_m)\frac{a}{2} \tag{12}$$

It is noted that the positive real number k ($0 \leq k < \infty$) is the power law or volume fraction index, and z is the distance from the mid-plane of the FG plate. The FG plate becomes a fully ceramic plate when k is set to zero and fully metal for large value of k.

Thus, the Young's modulus (E) and material density (ρ) equations of the imperfect FGM plate can be expressed as (Ait Athmane *et al*. 2015, Ait Yahia *et al*. 2015, Hadji *et al*. 2015)

$$\begin{aligned} E(z) &= \left(E_c - E_m\right)\left(\frac{z}{h} + \frac{1}{2}\right)^k + E_m - \left(E_c - E_m\right)\frac{a}{2} \\ \rho(z) &= \left(\rho_c - \rho_m\right)\left(\frac{z}{h} + \frac{1}{2}\right)^k + \rho_m - \left(\rho_c - \rho_m\right)\frac{a}{2} \end{aligned} \tag{13}$$

However, Poisson's ratio (ν) is assumed to be constant. The material properties of a perfect FG plate can be obtained when α is set to zero.

2.3 Governing equations and boundary conditions

The equilibrium equations are derived by using the virtual work principle, which can be written for the plate as

$$\int_{-\frac{h}{2}}^{+\frac{h}{2}}\int_{\Omega} (\sigma_x \delta\varepsilon_x + \sigma_y \delta\varepsilon_y + \tau_{xy}\delta\gamma_{xy} + \tau_{yz}\delta\gamma_{yz} + \tau_{xz}\delta\gamma_{xz}).d\Omega.dz - \int_{\Omega} q.\delta w.d\Omega = 0 \tag{14}$$

where Ω is the top surface.

Substituting Eqs. (7) and (8) into Eq. (14) and integrating through the thickness of the plate, Eq. (14) can be rewritten as (Hassaine Daouadji *et al*. 2012)

$$\begin{aligned} &\int_{\Omega} (N_x.\delta\varepsilon_x^0 +_x + N_y.\delta\varepsilon_y^0 + N_{xy}.\delta\gamma_{xy}^0 + M_x^b.\delta k_x^b + M_y^b.\delta k_y^b + M_{xy}^b.\delta k_{xy}^b + M_x^s.\delta k_x^s \\ &+ M_y^s.\delta k_y^s + M_{xy}^s.\delta k_{xy}^s + S_{yz}^s.\delta\gamma_{yz}^s + S_{xz}^s.\delta\gamma_{xz}^s)d\Omega - \int_{\Omega} q(\delta w + \delta w_b)d\Omega = 0 \end{aligned} \tag{15}$$

Where

$$\begin{Bmatrix} N_x, & N_y, & N_{xy}, \\ M_x^b, & M_y^b, & M_{xy}^b, \\ M_x^s, & M_y^s, & M_{xy}^s, \end{Bmatrix} = \int_{-\frac{h}{2}}^{+\frac{h}{2}} (\sigma_x, \sigma_y, \tau_{xy}) \begin{Bmatrix} 1 \\ z \\ f(z) \end{Bmatrix} dz \tag{16}$$

$$(S_{xz}^s, S_{yz}^s) = \int_{-\frac{h}{2}}^{+\frac{h}{2}} (\tau_{xz}, \tau_{yz}) g(z) dz \tag{17}$$

The governing equations of equilibrium can be derived from Eq. (18) by integrating the displacement gradients by parts and setting the coefficients δu_0, δv_0, δw_b, and δw_s zero separately. Thus, one can obtain the equilibrium equations associated with the present shear deformation theory.

$$\begin{cases} \delta u: \dfrac{\partial N_x}{\partial x} + \dfrac{\partial N_{xy}}{\partial y} = 0 \\ \delta v: \dfrac{\partial N_{xy}}{\partial x} + \dfrac{\partial N_y}{\partial y} = 0 \\ \delta w_b: \dfrac{\partial^2 M_x^b}{\partial x^2} + 2\dfrac{\partial^2 M_{xy}^b}{\partial x \partial y} + \dfrac{\partial^2 M_y^b}{\partial y^2} + q = 0 \\ \delta w_s: \dfrac{\partial^2 M_x^s}{\partial x^2} + 2\dfrac{\partial^2 M_{xy}^s}{\partial x \partial y} + \dfrac{\partial^2 M_y^s}{\partial y^2} + \dfrac{\partial S_{xz}^s}{\partial x} + \dfrac{\partial S_{yz}^s}{\partial y} + q = 0 \end{cases} \tag{18}$$

Using Eq. (8) in Eq. (16), the stress resultants of the plate can be related to the total strains by

$$\begin{Bmatrix} N \\ M^b \\ M^s \end{Bmatrix} = \begin{bmatrix} A & B & B^s \\ A & D & D^s \\ B^s & D^s & H^s \end{bmatrix} \begin{Bmatrix} \varepsilon \\ k^b \\ k^s \end{Bmatrix}; \qquad S = A^s \gamma \tag{19}$$

Where

$$N = \{N_x, N_y, N_{xy}\}^t, \quad M^b = \{M_x^b, M_y^b, M_{xy}^b\}^t, \quad M^s = \{M_x^s, M_y^s, M_{xy}^s\}^t \tag{20}$$

$$N = \{N_x, N_y, N_{xy}\}^t, \quad M^b = \{M_x^b, M_y^b, M_{xy}^b\}^t, \quad M^s = \{M_x^s, M_y^s, M_{xy}^s\}^t \tag{21}$$

$$A = \begin{bmatrix} A_{11} & A_{12} & 0 \\ A_{12} & A_{22} & 0 \\ 0 & 0 & A_{66} \end{bmatrix}, \quad B = \begin{bmatrix} B_{11} & B_{12} & 0 \\ B_{12} & B_{22} & 0 \\ 0 & 0 & B_{66} \end{bmatrix}, \quad D = \begin{bmatrix} D_{11} & D_{12} & 0 \\ D_{12} & D_{22} & 0 \\ 0 & 0 & D_{66} \end{bmatrix} \tag{22}$$

$$B^s = \begin{bmatrix} B_{11}^s & B_{12}^s & 0 \\ B_{12}^s & B_{22}^s & 0 \\ 0 & 0 & B_{66}^s \end{bmatrix}, \quad D^s = \begin{bmatrix} D_{11}^s & D_{12}^s & 0 \\ D_{12}^s & D_{22}^s & 0 \\ 0 & 0 & D_{66}^s \end{bmatrix}, \quad H^s = \begin{bmatrix} H_{11}^s & H_{12}^s & 0 \\ H_{12}^s & H_{22}^s & 0 \\ 0 & 0 & H_{66}^s \end{bmatrix} \tag{23}$$

$$S = \{S_{xz}^z, S_{yz}^s\}^t, \qquad \gamma = \{\gamma_{xz}, \gamma_{yz}\}^t, \qquad A^s = \begin{bmatrix} A_{44}^s & 0 \\ 0 & A_{55}^s \end{bmatrix} \tag{24}$$

The stiffness coefficients A_{ij} and B_{ij}, etc., are defined as

$$\begin{Bmatrix} A_{11} & B_{11} & D_{11} & B_{11}^s & D_{11}^s & H_{11}^s \\ A_{12} & B_{12} & D_{12} & B_{12}^s & D_{12}^s & H_{12}^s \\ A_{66} & B_{66} & D_{66} & B_{66}^s & D_{66}^s & H_{66}^s \end{Bmatrix} = \int_{-\frac{h}{2}}^{+\frac{h}{2}} Q_{11}(1, z, z^2, f(z), zf(z), f^2(z)) \begin{Bmatrix} 1 \\ \nu \\ \dfrac{1-\nu}{2} \end{Bmatrix} dz \tag{25}$$

$$(A_{22}, B_{22}, D_{22}, B_{22}^s, D_{22}^s, H_{22}^s) = (A_{11}, B_{11}, D_{11}, B_{11}^s, D_{11}^s, H_{11}^s), \qquad Q_{11} = \frac{E(z)}{1-\mu^2} \tag{26}$$

$$A_{44}^s = A_{55}^s = \int_{-\frac{h}{2}}^{+\frac{h}{2}} \frac{E(z)}{2(1+\nu)} [g(z)]^2 dz \tag{27}$$

Substituting from Eq. (16) into Eq. (18), we obtain the following equation (Hassaine Daouadji *et al*. 2012)

$$\begin{aligned} &A_{11}d_{11}u_0 + A_{66}D_{22}u_0 + (A_{12} + A_{66})d_{12}v_0 - B_{11}d_{11}w_b - (B_{12} + 2B_{66})d_{122}w_b \\ &-(B_{12}^s + 2B_{66}^s)d_{122}w_s - B_{11}^s d_{111}w_s = 0 \end{aligned} \tag{28}$$

$$\begin{aligned} &A_{22}d_{22}v_0 + A_{66}d_{11}v_0 + (A_{12} + A_{66})d_{12}u_0 - B_{22}d_{222}w_b - (B_{12} + 2B_{66})d_{112}w_b \\ &-(B_{12}^s + 2B_{66}^s)d_{112}w_s - B_{22}^s d_{222}w_s = 0 \end{aligned} \tag{29}$$

$$\begin{aligned} &B_{11}d_{111}u_0 + (B_{12} + 2B_{66})d_{122}u_0 + (B_{12} + 2B_{66})d_{112}v_0 + B_{22}d_{222}v_0 - D_{11}d_{1111}w_b \\ &-2(D_{12} + 2D_{66})d_{1122}w_b - D_{22}d_{2222}w_b - D_{11}^s d_{1111}w_s - 2(D_{12}^s + 2D_{66}^s)d_{1122}w_s \\ &-D_{22}^s d_{2222}w_s + q = 0 \end{aligned} \tag{30}$$

$$\begin{aligned} &B_{11}^s d_{111}u_0 + (B_{12}^s + 2B_{66}^s)d_{122}u_0 + (B_{12}^s + 2B_{66}^s)d_{112}v_0 + B_{22}^s d_{222}v_0 - D_{11}^s d_{1111}w_b \\ &-2(D_{12}^s + 2D_{66}^s)d_{1122}w_b - D_{22}^s d_{2222}w_b - H_{11}^s d_{1111}w_s - 2(H_{12}^s + 2H_{66}^s)d_{1122}w_s \\ &-H_{22}^s d_{2222}w_s + A_{55}^s d_{11}w_s + A_{44}^s d_{22}w_s + q = 0 \end{aligned} \tag{31}$$

Where d_{ij}, d_{ijl}, and d_{ijlm} are the following differential operators

$$d_{ij} = \frac{\partial^2}{\partial x_i \partial x_j}, \quad d_{ijl} = \frac{\partial^3}{\partial x_i \partial x_j \partial x_l}, \quad d_{ijlm} = \frac{\partial^4}{\partial x_i \partial x_j \partial x_l \partial x_m}, \qquad (i, j, l, m = 1, 2) \tag{32}$$

3. Results and discussion

In numerical analysis, fundamental frequencies of simply supported perfect and imperfect FG Plates are evaluated. The FG plate is taken to be made of aluminum and alumina with the following material properties:

Ceramic (P_C: Alumina, Al_2O_3): E_c = 380 GPa;

Metal (P_M: Aluminium, Al): E_m = 70 GPa; ν = 0.3;

And their properties change through the thickness of the plate according to power-law. The bottom surfaces of the FG plate are aluminum rich, whereas the top surfaces of the FG plate are alumina rich.

For convenience, the following dimensionless form is used

$$\bar{w}=10\frac{E_C h^3}{q_0 a^4}w\left(\frac{a}{2},\frac{b}{2}\right),\qquad \bar{u}=100\frac{E_C h^3}{q_0 a^4}u\left(0,\frac{b}{2},\frac{-h}{4}\right),\qquad \bar{v}=100\frac{E_C h^3}{q_0 a^4}v\left(\frac{a}{2},0,\frac{-h}{6}\right)$$
$$\bar{\sigma}_x=\frac{h}{hq_0}\sigma_x\left(\frac{a}{2},\frac{b}{2},\frac{h}{2}\right),\qquad \bar{\sigma}_y=\frac{h}{hq_0}\sigma_y\left(\frac{a}{2},\frac{b}{2},\frac{h}{3}\right),\tag{33}$$
$$\bar{\tau}_{xy}=\frac{h}{hq_0}\tau_{xy}\left(0,0,-\frac{h}{3}\right),\qquad \bar{\tau}_{xz}=\frac{h}{hq_0}\tau_{xz}\left(0,\frac{b}{2},0\right),\qquad \bar{\tau}_{yz}=\frac{h}{hq_0}\tau_{yz}\left(\frac{a}{2},0,\frac{h}{6}\right).$$

To validate accuracy of the refined plate theory, the comparisons between the present results and the available results obtained by Reddy (2000), Karama (Karama *et al*. 2003), Hassaine Daouadji (2012) and the 3D solutions of Werner (1999).

Table 1 Center deflections of isotropic homogenous plates (k = 0, $E_m = E_C = E$ = 1 and a/b = 1)

a/h	Karama (ESDPT)	Reddy (PSDPT)	Hassaine Daouadji (NHPSDT)	3D (Z = 0)	Present theory (RSDPT)		
	α = 0	α = 0	α = 0	α = 0	α = 0	α = 0.1	α = 0.2
0.01	44380.05	44383.88	44383.86	44384.7	44383.84	49315.39	55479.80
0.1	46.2763	46.6588	46.65655	46.7443	46.65480	51.83867	58.3185

Table 2 Comparison of normalized displacements and stresses of a FGM rectangular plate (b = 3a and k = 2)

a/h	Theory	α	w	σ_x	σ_y	τ_{yz}	τ_{xz}	τ_{xy}
4	ESDPT	α = 0	4.0569	5.2804	0.6644	0.6084	0.6699	0.5900
	PSDPT	α = 0	4.0529	5.2759	0.6652	0.6058	0.6545	0.5898
	Present theory	α = 0	3.8716	5.4197	0.66778	0.6096	0.6802	0.5395
		α = 0.1	4.7346	5.9455	0.6796	0.6312	0.6717	0.4940
		α = 0.2	6.2567	6.8649	0.6809	0.6598	0.6624	0.4148
10	ESDPT	α = 0	3.5543	12.9252	1.6938	0.61959	0.6841	1.4898
	PSDPT	α = 0	3.5537	12.9234	1.6941	0.6155	0.6672	1.4898
	Present theory	α = 0	3.5231	12.9841	1.6995	0.6211	0.6922	1.4659
		α = 0.1	4.3921	14.2925	1.7073	0.6431	0.6821	1.3695
		α = 0.2	5.9992	16.6660	1.7174	0.6723	0.6679	1.1948
20	ESDPT	α = 0	3.4824	25.7712	3.3971	0.6214	0.6878	2.9844
	PSDPT	α = 0	3.48225	25.7703	3.3972	0.6171	0.6704	2.9844
	Present theory	α = 0	3.4745	25.8012	3.4001	0.6231	0.6951	2.9719
		α = 0.1	4.3452	28.4167	3.4167	0.6452	0.6845	2.7851
		α = 0.2	5.9665	33.1876	3.4388	0.6745	0.6687	2.4428
100	ESDPT	α = 0	3.4593	128.728	17.0009	0.6220	0.6894	14.9303
	PSDPT	α = 0	3.45937	128.7283	17.0009	0.6177	0.67176	14.9303
	Present theory	α = 0	3.4591	128.734	17.0015	0.6238	0.6962	14.9278
		α = 0.1	4.3305	141.8106	17.0863	0.6459	0.6854	14.0039
		α = 0.2	5.9566	165.7058	17.2002	0.6752	0.6689	12.3036

The present solution is realized for a quadratic plate in table 1, with the following fixed data: $a = 1$, $b = 1$, $E_m = E_c = E = 1$, $q_0 = 1$, $v = 0.3$ and two values for the plate thickness: $h = 0.01$, $h = 0.1$ It is to be noted that the present results of the center deflection compare very well with the 3-D solution for perfect FG plate and takes maximum values for the imperfect FG plate ($\alpha = 0.1$ and $\alpha = 0.2$). This is expected because the imperfect FG plate is the one with the lowest stiffness and the perfect FG plate is the one with the highest stiffness.

The center deflection $\overline{w}$ and the distribution across the plate thickness of in-plane longitudinal stress $\overline{\sigma}_x$ and longitudinal tangential stress $\overline{\tau}_{xy}$ are shown in Table 2 for different values of the plate thickness a/h. It is to be noted that the present results compare very well with the other theories solution. In addition the comparisons show that the effect of the porosity on the deflection of FG plates with two different type of porosity. The results reveal that the deflection results increase as the volume fraction of porosity (α) increases.

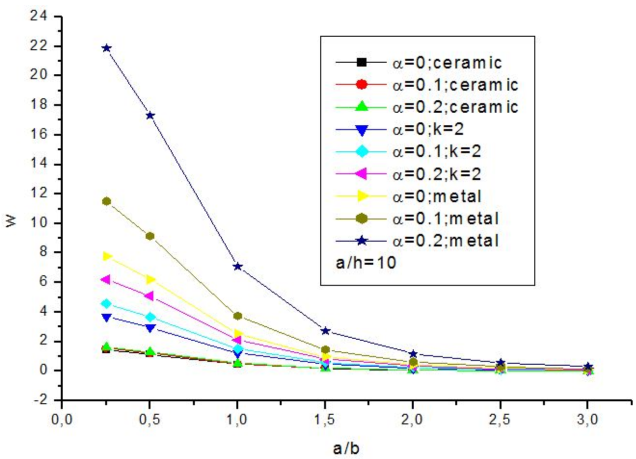

Fig. 1 Dimensionless center deflection (w) as function of the aspect ratio (a/b) of a perfect and imperfect FGM plate

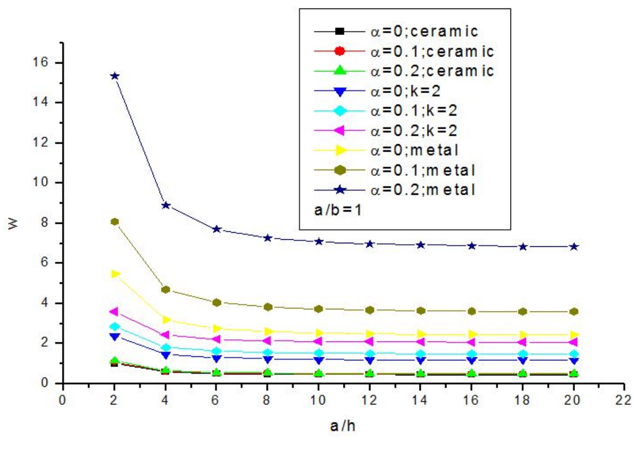

Fig. 2 Dimensionless center deflection (w) as a function of the side-to-thickness ratio (a/h) of a perfect and imperfect FGM square plate

Figs. 1 and 2 shows the variation of the non-dimensional deflection with the aspect and side-to-thickness ratio, respectively for simply supported perfect and imperfect FG plates based on the present plate theory. The deflection is maximum for the imperfect FG plate (α = 0.1 and α = 0.2) and minimum for the perfect FG plate (α = 0). The difference increases as the aspect ratio increases while it may be unchanged with the increase of side-to-thickness ratio.

For both material pairs, the non-dimensional deflection of the metallic plate is found to be of the largest values and that of the ceramic plate, of the smallest values. All the plates with intermediate properties undergo corresponding intermediate values of the non-dimensional deflection. This is expected because the metallic plate is the one with the lowest stiffness and the ceramic plate is the one with the highest stiffness.

Figs. 3 and 4 contains the plots of the in-plane longitudinal and normal stresses $\overline{\sigma}_x$ and $\overline{\sigma}_y$ through-the-thickness of the perfect and imperfect FG plate for k = 2. The stresses are tensile at the

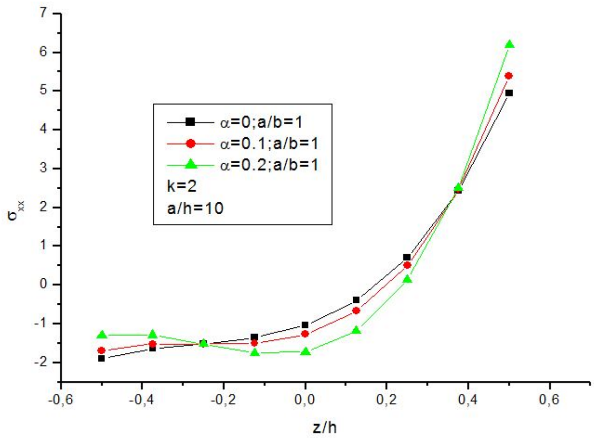

Fig. 3 Variation of in-plane longitudinal stress (σ_{xx}) through-the thickness of an FGM plate for different values of the volume fraction of porosity

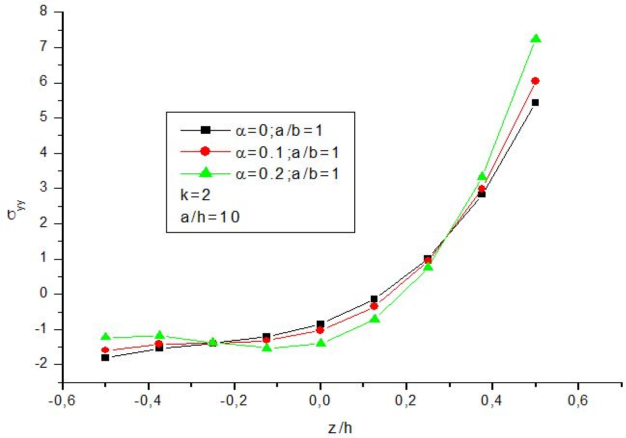

Fig. 4 Variation of in-plane normal stress (σ_{yy}) through-the thickness of an FGM plate for different values of the volume fraction of porosity

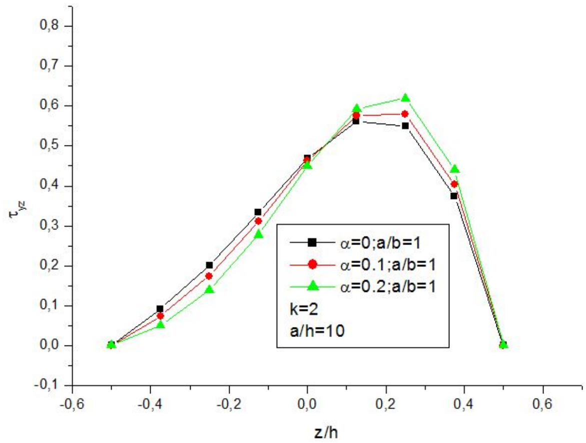

Fig. 5 Variation of transversal shear stress τ_{yz} through-the thickness of an FGM plate for different values of the volume fraction of porosity

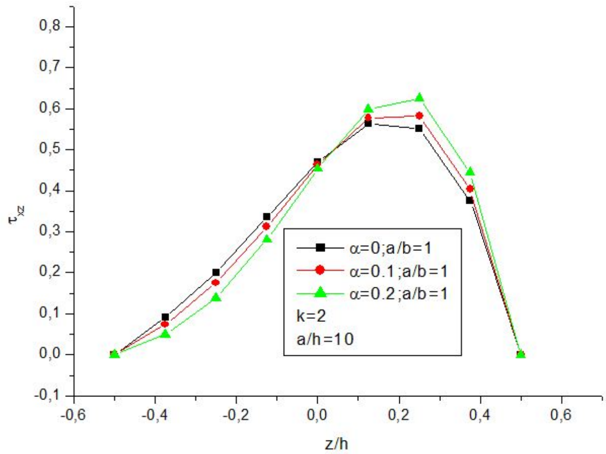

Fig. 6 Variation of transversal shear stress τ_{xz} through-the thickness of an FGM plate for different values of the volume fraction of porosity

top surface and compressive at the bottom surface and take the maximum values for the imperfect FG plate.

Figs. 5 and 6, shows the distribution of the shear stresses $\bar{\tau}_{xz}$ and $\bar{\tau}_{yz}$ through the thickness of the FG Plate. The volume fraction exponent of the FG plate in taken as $k = 2$. It's clear that the distributions are not parabolic and the stresses increase for the imperfect FG plate.

4. Conclusions

A new refined shear deformation plate theory is proposed for static analysis of perfect and imperfect FG plates. The theory accounts for parabolic distribution of the transverse shear strains and satisfies the zero traction boundary conditions on the surfaces of the plate without using shear correction factors. The modified rule of mixture covering porosity phases is used to describe and approximate material properties of the imperfect FG plates. Based on the present plate theory, the equilibrium equations are derived from the principle of virtual displacements. The influence of the porosities on deflection and stresses is then discussed. Numerical examples show that the proposed theory gives solutions which are almost identical with those obtained using other shear deformation theories.

Acknowledgments

The authors thank the referees for their valuable comments.

References

Ait Atmane, H., Tounsi, A. and Bernard, F. (2015), "Effect of thickness stretching and porosity on mechanical response of a functionally graded beams resting on elastic foundations", *Int. J. Mech. Mater.*, 1-14.

Ait Yahia, S., Ait Atmane, H., Sid Ahmed Houari, M. and Tounsi, A. (2015), "Wave propagation in functionally graded plates with porosities using various higher-order shear deformation plate theories", *Struct. Eng. Mech., Int. J.*, **53**(6), 1143-1165.

Al-Basyouni, K.S., Tounsi, A. and Mahmoud, S.R. (2015), "Size dependent bending and vibration analysis of functionally graded micro beams based on modified couple stress theory and neutral surface position", *Compos. Struct.*, **125**, 621-630.

Bennoun, M., Houari, M.S.A. and Tounsi, A. (2016), "A novel five variable refined plate theory for vibration analysis of functionally graded sandwich plates", *Mech. Adv. Mater. Struct.*, **23**(4), 423-431.

Bourada, M., Kaci, A., Houari, M.S.A. and Tounsi, A. (2015), "A new simple shear and normal deformations theory for functionally graded beams", *Steel Compos. Struct., Int. J.*, **18**(2), 409-423.

Carrera, E., Brischetto, S., Cinefra, M. and Soave, M. (2010), "Refined and advanced models for multilayered plates and shells embedding functionally graded material layers", *Mech. Adv. Mater. Struct.*, **17**(8), 603-621.

Cinefra, M., Carrera, E., Della Croce, L. and Chinosi, C. (2012), "Refined shell elements for the analysis of functionally graded structures", *Compos. Struct.*, **94**(2), 415-422.

Hadji, L., Hassaine Daouadji, T. and Adda Bedia, E.A. (2015), "A refined exponential shear deformation theory for free vibration of FGM beam with porosities", *Geomech. Eng., Int. J.*, **9**(3), 361-372.

Hassaine Daouadji, T., Tounsi, A., Hadji, L., Hadj, H.A. and El Abbes, A.B. (2012), "A theoretical analysis for static and dynamic behavior of functionally graded plates", *Mater. Phys. Mech.*, **14**, 110-128.

Karama, M., Afaq, K.S. and Mistou, S. (2003), "Mechanical behavior of laminated composite beam by the new multi-layered laminated composite structures model with transverse shear stress continuity", *Int. J. Solids Struct.*, **40**(6), 1525-1546.

Kiani, Y., Akbarzadeh, A.H., Chen, Z.T. and Eslami, M.R. (2011), "Static and dynamic analysis of an FGM doubly curved panel resting on the Pasternak-type elastic foundation", *Compos. Struct.*, **94**(8), 2474-2484.

Koizumi, M. (1997), "FGM activities in Japan", *Compos. Part B*, **28**(1-2), 1-4.

Loy, C.T., Lam, K.Y. and Reddy, J.N. (1999), "Vibration of functionally graded cylindrical shells", *Int. J. Mech. Sic.*, **41**(3), 309-324.

Mahi, A., Adda Bedia, E.A. and Tounsi, A. (2015), "A new hyperbolic shear deformation theory for bending and free vibration analysis of isotropic, functionally graded, sandwich and laminated composite plates", *Appl. Math. Model.*, **39**(9), 2489-2508.

Neves, A.M.A., Ferreira, A.J.M., Carrera, E., Roque, C.M.C., Cinefra, M., Jorge, R.M.N. and Soares, C.M.M. (2011), "Bending of FGM plates by a sinusoidal plate formulation and collocation with radial basis functions", *Mech. Res. Commun.*, **38**(5), 368-371.

Neves, A.M.A., Ferreira, A.J.M., Carrera, E., Cinefra, M., Roque, C.M.C., Jorge, R.M.N. and Soares, C.M.M. (2012a), “A quasi-3D hyperbolic shear deformation theory for the static and free vibration analysis of functionally graded plates”, *Compos*. *Struct*., **94**(5), 1814-1825.

Neves, A.M.A., Ferreira, A.J.M., Carrera, E., Roque, C.M.C., Cinefra, M., Soares, C.M.M. and Jorge, R.M.N. (2012b), “A quasi-3D sinusoidal shear deformation theory for the static and free vibration analysis of functionally graded plates”, *Compos*. *Part B*, **43**(2), 711-725.

Ravikiran, K., Kashif, A. and Ganesan, G. (2008), “Static analysis of functionally graded beams using higher order shear deformation theory”, *Appl*. *Math*. *Model*., **32** (12), 2509-2525.

Ravikiran, K., Kashif, A. and Ganesan, N. (2013), “Static analysis of functionally graded beams using higher order shear deformation theory”, *Appl*. *Math*. *Model*., **32**(12), 2509-2525.

Reddy, J.N. (1984), “A simple higher-order theory for laminated composite plates”, *J*. *Appl*. *Mech*., **51**(4), 745-752.

Reddy, J.N. (2000), “Analysis of functionally graded plates”, *Int*. *J*. *Numer*. *Method*. *Eng*., **47**(1-3), 663-684.

Sepahi, O., Forouzan, M.R. and Malekzadeh, P. (2008), “Large deflection analysis of thermo-mechanical loaded annular FGM plates on nonlinear elastic foundation via DQM”, *Compos*. *Struct*., **92**(10), 2369-2378.

Sepahi, O., Forouzan, M.R. and Malekzadeh, P. (2010), “Large deflection analysis of thermo-mechanical loaded annular FGM plates on nonlinear elastic foundation via DQM”, *Compos*. *Struct*., **92**(10), 2369-2378.

Sid Ahmed Houari, M., Tounsi, A. and Anwar Bég, O. (2013), “Thermoelastic bending analysis of functionally graded sandwich plates using a new higher order shear and normal deformation theory”, *Int*. *J*. *Mech*. *Sci*., **76**, 102-111.

Wattanasakulpong, N. and Ungbhakorn, V. (2014), “Linear and nonlinear vibration analysis of elastically restrained ends FGM beams with porosities”, *Aerosp*. *Sci*. *Technol*., **32**(1), 111-120.

Wattanasakulpong, N., Prusty, B.G., Kelly, D.W. and Hoffman, M. (2012), “Free vibration analysis of layered functionally graded beams with experimental validation”, *Mater*. *Des*., **36**, 182-190.

Werner, H. (1999), “A three-dimensional solution for rectangular plate bending free of transversal normal stresses”, *Numer*..*Method*..*Eng*., **15**(4), 295-302.

Zhu, J., Lai, Z., Yin, Z., Jeon, J. and Lee, S. (2001), “Fabrication of ZrO_2–NiCr functionally graded material by powder metallurgy”, *Mater*. *Chem*. *Phys*., **68**(1-3), 130-135.

CC